Eur. Phys. J. B **58**, 373–378 (2007)
DOI: 10.1140/epjb/e2007-00242-0

THE EUROPEAN PHYSICAL JOURNAL B

Improvement of the intergranular pinning energy in uniaxially compacting (Bi-Pb)$_2$Sr$_2$Ca$_2$Cu$_3$O$_{10+\delta}$ ceramic samples

E. Govea-Alcaide[1,2,a], I. García-Fornaris[3], P. Muné[1], and R.F. Jardim[2]

[1] Departamento de Física, Universidad de Oriente, Patricio Lummumba s/n, P.O. Box 90500, Santiago de Cuba, Cuba
[2] Instituto de Física, Universidade de São Paulo, CP 66318, 05315-970, S. Paulo, SP, Brazil
[3] Departamento de Ciencias Básicas, Universidad de Granma, Apdo. 21, P.O. Box 85100, Bayamo, Cuba

Received 27 March 2007/ Received in final form 4 August 2007
Published online 14 September 2007 –

Abstract. Measurements of the electrical resistivity as a function of temperature, $\rho(T)$, for different values of applied magnetic field, B_a ($0 \leq B_a \leq 50$ mT), were performed in polycrystalline samples of $Bi_{1.65}Pb_{0.35}Sr_2Ca_2\ Cu_3O_{10+\delta}$ subjected to different uniaxial compacting pressure (UCP). We have found appreciable differences in the grain orientation between samples by using X-ray diffractometry. From the X-ray diffraction patterns performed, in powder and pellet samples, we have estimated the Lotgering factor along the $(00l)$ direction, $F_{(00l)}$. The results indicate that $F_{(00l)}$ increases ∼23% with increasing UCP suggesting that grains of these samples are preferentially aligned along the c-axis, which is parallel to the compacting direction. The resistive transition of the samples have been interpreted in terms of the thermally activated flux-creep model. In addition, the effective intergranular pinning energy, U_0, have been determined for different applied magnetic field. The magnetic field dependence of U_0, for $B_a > 8$ mT, was found to follow a $H^{-\alpha}$ dependence with $\alpha = 0.5$ for all samples. The analysis of the experimental data strongly suggested that increasing UCP results in appreciable changes in both the grain alignment and the grain connectivity of the samples. We have successfully interpreted the data by considering the existence of three different superconducting levels within the samples: the superconducting grains, the weak-links, and the superconducting clusters.

PACS. 74.72.Hs Bi-based cuprates – 74.81.Bd Granular, melt-textured, amorphous and composite superconductors – 74.25.Fy Transport properties (electric and thermal conductivity, thermoelectric effects, etc.) – 74.25.Qt Vortex lattices, flux pinning, flux creep

1 Introduction

The broadening of the $\rho(T)$ transition of type-II superconductors in applied magnetic fields, B_a, has been extensively investigated for many years [1–5]. There is consensus that the width of the superconducting transition is strongly influenced by the anisotropy associated with the orientation of the applied magnetic field respect to the Cu-O planes [6–8]. Several models such as: superconducting glass [9], flux-flow [1], flux-creep [2], Ambegaokar — Halperin [10], Kosterlitz — Thouless transition [11], Josephson coupling [3], thermally activated flux flow [12], etc. Notice that, most of these models invoke the flux motion as the source of the dissipation in these materials.

In polycrystalline high-T_c superconductors, where the transport properties are mostly determined by its granular nature, the above physical scenario becomes much more complex. The presence of current-path frustration such as voids, cracks, and grain boundaries in these samples is an unavoidable fact mostly to the virtue of the preparation process employed that results in ceramic materials. Grain boundaries play an important role in limiting the transport properties of polycrystalline superconductors. Moreover, it is well established that the properties of the grain boundaries control much of the macroscopic superconducting properties of all high-T_c materials [13]. It is believed that this phenomenon is mainly due to the misorientation between grains [14]. High angle grain boundaries act as Josephson coupled weak-links, leading to a significant field-dependent suppression of the supercurrent across the boundary [13]. A way to improve the transport properties of these materials is to subjected them to large mechanical deformations.

Previously, Muné et al. have described studies concerning the influence of uniaxial compacting pressure (UCP) on the general superconducting properties in (Bi-Pb)$_2$Sr$_2$ Ca$_2$Cu$_3$O$_{10+\delta}$ (Bi-2223) ceramic samples subjected to different UCP ranging from 90 to 600 MPa [15]. By

[a] e-mail: egovea@cnt.uo.edu.cu

performing measurements of critical current density as function of applied magnetic field $J_c(B_a)$, three different superconducting levels have been identified: the superconducting grains, the superconducting clusters, and the weak-links [15]. Magneto-optical images in combination with numerical methods have confirmed the existence of those different superconducting levels within a polycrystalline $YBa_2Cu_3O_{7-\delta}$ sample [16]. It was also found that properties of the last two levels are very sensitive to the compacting pressure, mostly due to changes in the grain boundary properties. Under these conditions, it is believed that the flux motion comprises the dynamics of three kind of vortices: the Abrikosov vortices (A), the Abrikosov-Josephson vortices (A-J) [17], and the Josephson vortices (J), respectively. Fortunately, under certain external conditions the flux dynamics is mainly dominated by only one kind of these vortices [18]. It is believed that, in low applied magnetic field the flux dynamics is dominated by both A-J and J vortices. In this case, the A-J vortices in the low-angle grain boundaries and the latter in the high-angle grain boundaries or weak-links [17]. On the other hand, it is expected that the Abrikosov vortex dynamics is manifested for high applied magnetic fields [19].

In this work we focus on the electrical resistive transition in low applied magnetic field ($B_a < 20$ mT) of $Bi_{1.65}Pb_{0.35}Sr_2$ $Ca_2Cu_3O_{10+\delta}$ ceramic samples subjected to different UCP ranging from 100 to 250 MPa. X-ray diffraction (XRD), taken on powder and bulk samples has been performed as a complementary characterization. The main contribution of the paper is to present a systematic study of the effective intergranular pinning energy as a function of the applied magnetic field in samples with similar intragranular properties, but different intergranular properties.

2 Experimental

Polycrystalline samples of $Bi_{1.65}Pb_{0.35}Sr_2Ca_2$ $Cu_3O_{10+\delta}$ (Bi-2223) were prepared from powders of Bi_2O_3, PbO, $SrCO_3$, $CaCO_3$, and CuO, which were mixed in an atomic ratio of Pb:Bi:Sr:Ca:Cu (0.35:1.65:2:2:3). Details of the sample preparation process are described elsewhere [15]. Then, before the last heat treatment, the obtained powders were uniaxially pressed at different compacting pressures ranging from 100 to 250 MPa. The typical dimensions of the pellets were $d = 15$ mm in diameter and $h = 1$ mm in height. The last heat treatment was performed in air at 845 °C for 40 h followed by slow cooling.

We have evaluated the phase identification in both powder and bulk samples by means of X-ray diffraction patterns obtained in a Bruker-AXS D8 Advance diffractometer. These measurements were performed at room temperature using Cu Kα radiation in the $3° \leq 2\theta \leq 80°$ range with a 0.05° (2θ) step size and 5 s counting time.

The temperature dependence of the electrical resistivity for different values of applied magnetic field, $\rho(T, B_a)$, was measured by using the standard dc four-probe technique. Before each measurement, the samples were cooled from room temperature down to 77 K. Then, a magnetic field B_a was applied always perpendicular to the thickness and to the excitation current, that was injected along the major length of samples. Both the voltage across the sample and its temperature were collected while the temperature was raised slowly to 300 K. The typical dimensions of samples are $t = 1$ mm (thickness), $w = 2$ mm (width), and $l = 10$ mm (length). Also, the excitation current in our measurements was 1 mA ($J \sim 5 \times 10^{-2}$ A/cm^2).

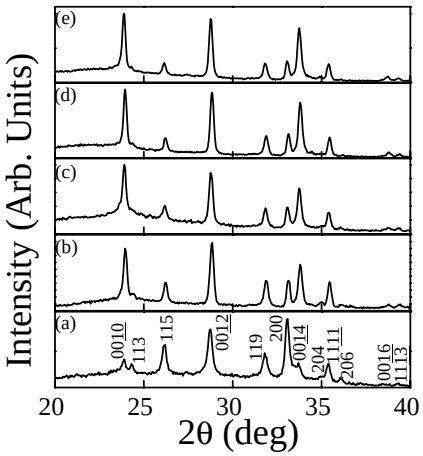

Fig. 1. X-ray diffraction patterns of a powder sample (a), and bulk samples **BP2** (b), **BP3** (c), **BP4** (d), and **BP5** (e). The reflections belonging to the Bi-2223 phase are marked by Miller indexes in (a).

Measurements of superconducting critical current density dependence on applied magnetic field, $J_c(B_a)$, were performed by the same dc technique as in $\rho(T)$ measurement. Here, the so-called *virgin curve* is obtained by cooling the sample from room temperature down to 77 K under zero applied magnetic field. Then, the magnetic field is increased from zero to a fixed value B_a. Once the magnetic field is set, the excitation current, I, through the sample is increased automatically and the voltage across the sample is measured. Under these circumstances, we have extracted the $J_c(B_a)$ value from the measured I versus V curve, by taking the J_c value as the excitation current density in which the voltage across the sample reaches values of 1 μV. This procedure is repeated several times for different fixed values of B_a in the 0–7 mT range. From the values of J_c obtained at different B_a, we are able to obtain the $J_c(B_a)$ dependence for increasing applied magnetic fields.

3 Results and discussion

Figure 1 displays the X-ray diffraction patterns taken on bulk samples **BP2**, **BP3**, **BP4**, and **BP5**. The results shown in this figure indicate that all samples have similar chemical composition and that all the indexed reflections are related to the high-T_c Bi-2223 phase. The unit-cell parameters were calculated with respect to an orthorhombic unit cell and the obtained values $a = 5.410$ Å, $b = 5.413$ Å, and $c = 37.152$ Åare very similar to those reported elsewhere for the same compound [20]. We have also found that values of a,

Table 1. Few parameters of the samples studied in this work: the compacting pressure, P, the Lotgering factor along $(00l)$ direction, $F_{(00l)}$, the onset superconducting critical temperature, T_{on}, the offset superconducting critical temperature, T_{off}, the effective intergranular pinning energy U_0, and the transport critical current density at zero applied magnetic field, $J_c(0)$.

Sample	P (MPa)	$F_{(00l)}$	T_{on} (K)	T_{off}(0 mT) (K)	T_{off}(16 mT) (K)	U_0(1 mT) (eV)	U_0(16 mT) (eV)	$J_c(0)$ (A/cm^2)
BP2	99	0.54	119.5	98	86	2.1	0.63	42
BP3	148	0.63	119.7	102	94	3.2	0.65	293
BP4	198	0.64	120.1	104	98	6.7	0.80	461
BP5	247	0.70	120.2	105	99	7.5	0.87	547

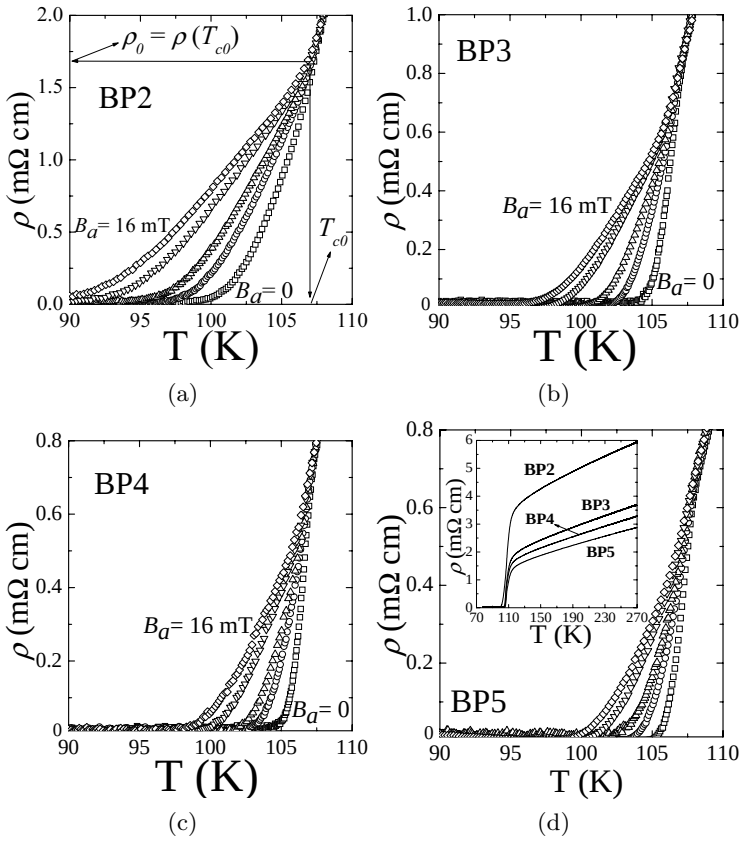

Fig. 2. Resistive transition of samples **BP2** (a), **BP3** (b), **BP4** (c), and **BP5** (d) for $B_a = 0$, 2, 4, 8, and 16 mT. In (a), ρ_0 is the electrical resistivity at $T = T_{c0}$ and T_{c0} is the temperature where the resistivity curves for different applied magnetic field, separate each one. Also, the complete temperature dependence of $\rho(T)$ between 77 and 270 K, for each sample, are shown in the insert of (d).

b, and c were similar for all samples subjected to different compacting pressures. As reported previously, is a characteristic of Bi-based materials the occurrence of grains with platelet-like structure [15,21,22]. This Kind of morphology allows the orientation of the grains with it c-axis ($(00l)$ crystallographic plane) parallel to the compacting direction [15,21,23]. In order to evaluate the orientation degree of the $(00l)$ planes, we calculated the Lotgering factor, $F_{(00l)}$, by using the expression [24,25]:

$$F_{(00l)} = \frac{P - P_0}{1 - P_0}, \qquad (1)$$

where $P_0 = I_{0(00l)}/\sum I_{0(hkl)}$ and $P = I_{(00l)}/\sum I_{(hkl)}$. Here, $I_{0(00l)}$ and $I_{0(hkl)}$ are the intensities of $(00l)$ and (hkl) peaks for a powder sample, respectively. On the other hand, $I_{(00l)}$ and $I_{(hkl)}$ are the intensities of $(00l)$ and (hkl) peaks, respectively, for a pellet sample. Values of $F_{(00l)}$ are in the range 0 (non-oriented samples) to 1 (highly oriented samples). In this case, the obtained values of $F_{(00l)}$ are shown in Table 1. Notice that texture degree increase ∼30% between the sample **BP2** ($F_{(00l)} = 0.54$) and the sample **BP5** ($F_{(00l)} = 0.70$) with increasing the UCP. This not an unexpected result as reported elsewhere for the same materials [15,21,23]

In addition, all samples were also characterized by measurements of electrical resistivity versus temperature $\rho(T)$, for applied magnetic fields ranging from 0 to 16 mT, and the results are shown in Figure 2. The most

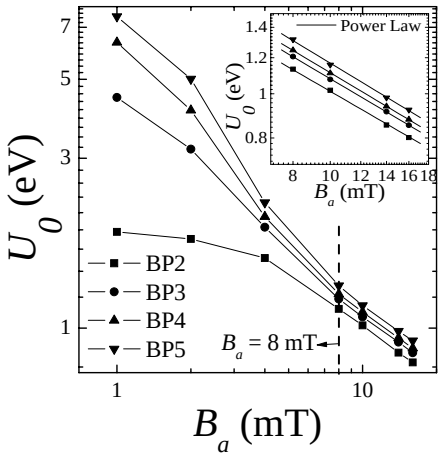

Fig. 3. The magnetic field dependence of the effective intergranular pinning energy, $U_0(H)$, for samples **BP2**, **BP3**, **BP4**, and **BP5**. Lines between points are guide for eyes. The insert shows an expanded view in the range between 7–18 mT. In this case the experimental data were fitting to the power law $U(H) \propto \mathrm{H}^{-\alpha}$ (see comments in the text).

important features of these can be summarized as follows: (a) all curves start to deviate from the linear behavior at high temperatures below the onset temperature $T_{on} \sim$ 120 K (please see values in Tab. 1), (b) the curves exhibit a linear dependence of $\rho(T)$ at high temperatures, $T_{on} >$ 120 K (see the insert of Fig. 2d), (c) the electrical resistivity at $T = 270$ K decrease ∼50% between 5.97 mΩ cm, in **BP2**, and between 2.89 mΩ cm, in **BP5**, (d) at $B_a = 0$ the temperature in which the zero resistance state is observed, T_{off} increase from 98 K in the sample **BP2** to 105 in **BP5**, and (e) at $B_a = 16$ mT T_{off} increase from 86 to 99, respectively, with increasing the uniaxial compacting pressure. Values of the offset temperature for each sample are shown in Table 1.

Notice that, the onset temperature is related to the transition of the isolated grains to the superconducting state and its constant value in all samples strongly suggests that the grains have similar stoichiometry. This result is in excellent agreement with those of XRD. On the other hand, T_{off} is related to volume fraction of the Bi-2223 phase and/or features of the intergranular component. Thus, as the chemical composition of grains are similar then the observed behavior of the offset temperature is just related to differences in the intergranular properties between samples. Additionally, the observed decrease of ρ(270 K) assures an increasing in both the grain connectivity and the texture degree of samples with the uniaxial compacting pressure [15,21].

A relevant point in our discussion is related to determine the influence of the UCP on the magnetic field dependence of the effective intergranular pinning energy, $U_0(H)$. In the framework of the thermally activated flux-creep model, which is an alternative to the Josephson-coupling model, the broadened resistivity curves for the

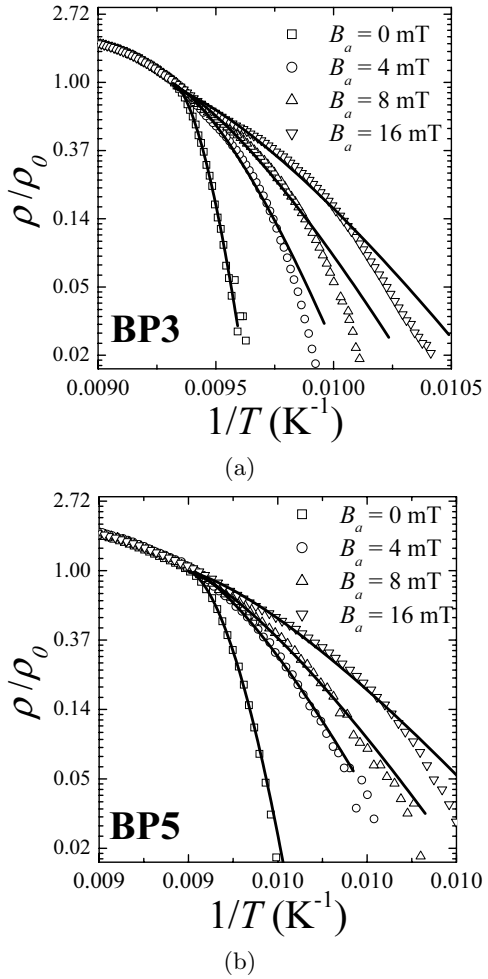

Fig. 4. Arrhenius plot for samples **BP3** and **BP5**. By fitting these curves to equation (2) is possible to obtain the value of the effective intergranular pinning energy for different applied magnetic fields, as discussed in the text.

high-T_c oxides superconductor can be expressed as:

$$\rho(T,H) = \rho_0 \exp\left(\frac{-U(H,T)}{T}\right), \qquad (2)$$

where $U(H,T) = U_0(H)(1-t)^q$ is the activation energy, $t = T/T_c$ the reduced temperature, q an exponential factor that vary between 1.5–1 in high-T_c materials [1–3], and ρ_0 the electrical resistivity at $T = T_{c0}$ with T_{c0} the temperature where the resistivity curves for different applied magnetic field, separate each other (see the Fig. 2a). Figure 3 displays the effective intergranular pinning energy as a function of applied magnetic field for samples **BP2**, **BP3**, **BP4**, and **BP5**. This energy is determined by fitting the $\rho(H,T)$ curve to equation (2). The obtained values of U_0 for 1 and 16 mT for are shown in Table 1. Also, values of T_{c0} and q are near 107.5 K and 1.6, respectively in all samples. In addition, Figure 4 shows examples of the Arrhenius plot for samples **BP3** and **BP5**.

As can be seen in Figure 3 the $U_0(H)$ dependence in all samples decreases as the magnetic field strength increases. The main differences between curves were observed for fields below 8 mT. Notice that this value is very close to a similar reported for the first critical field of grains, B_{c1g}, in Bi-2223 samples at $T = 77$ K [15,21]. Since below B_{c1g}, the applied magnetic field has penetrated only the intergranular media a possible interpretation for the differences between curves can be ascribed to the existence of different superconducting levels within the samples at the intergranular region: the superconducting grains, the weak-links, and the superconducting clusters [15,16]. As reported previously, the properties and the distribution of the last two levels are very sensitive to the compacting pressure of the samples. Thus, it would be reasonable to assure that in the sample **BP2**, the fraction of grains interconnected by strong-links (clusters) is very small as compared with the sample **BP5**. This suggests that in the former, the *"penetrable"* intergranular region by the external applied magnetic field is higher than in the latter. However, it seems that even in the sample **BP5**, where $F_{(00l)}$ is high, the number and/or the strength of superconducting clusters are not enough to avoid the magnetic field penetration. Notice that, the pinning energy increase ∼75% between **BP2** and **BP5** at $B_a = 1$ mT, while at $B_a = 8$ mT is only of ∼14% (see Tab. 1).

In order to complement the above statements, Figure 5 displays the experimental virgin curves of the normalized critical current density, $J_c(B_a)/J_c(0)$, as a function of applied magnetic of samples **BP2**, **BP3**, **BP4**, and **BP5**. Values of the critical current density at zero applied magnetic field, $J_c(0)$ are shown in Table 1. In this case, the results indicate that $J_c(0)$ increases ∼90% between sample **BP2** and **BP5**. Also, it was found that all curves have a behavior qualitatively similar. They show a clear Josephson-like behavior, in which $J_c(B_a)/J_c(0)$ dependence decreases with the increasing applied magnetic field. However, such a decrease is more marked in samples **BP2** and **BP3** where $J_c(B_a)/J_c(0)$ dependence decreases 90% and 86%, respectively, between 0 and 7 mT. In samples **BP4** and **BP5** the decrease is ∼70%. Notice that the behavior of the $J_c(B_a)$ dependence is strongly influenced by both intergranular and intragranular properties. The latter, according the analysis of both the X-ray diffraction patter and the $\rho(T)$ curves, is essentially the same for all samples. Thus as mentioned previously, it seems that the difference between our samples arises from changes in both the strength and the distribution of the intergranular media, i.e, the superconducting weak-links and the superconducting clusters. As a result in samples **BP2** and **BP3** the grains are mainly weakly connected to each other and the pinning energy is low. On the other hand, samples **BP4** and **BP5** are a little more homogeneous and the pinning energy is higher, as also suggested the results shown in Figure 3.

Finally, we want to point out that within the applied magnetic field range 0–8 mT, the functional dependence $U_0(H)$ do not follow the well-known form $U(H) \propto H^{-\alpha}$. This discrepancy is more pronounced in the curve of the sample **BP2**. However, it was found a better agreement to the typical power low for applied magnetic field greater than B_{c1g}. The value of α in all samples are very similar and close to 0.5, which are in excellent agreement with those found for high-T_c materials [2,26].

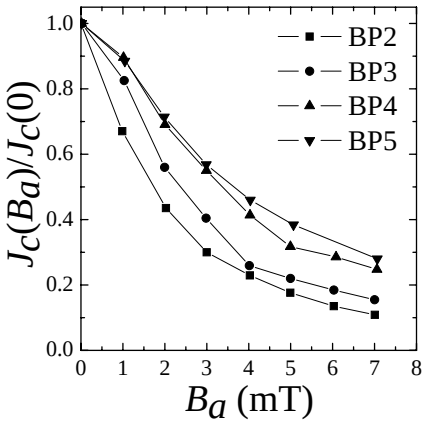

Fig. 5. The magnetic field dependence of the transport critical current density, $J_c(B_a)$, for samples **BP2**, **BP3**, **BP4**, and **BP5**. Lines between points are guide for eyes.

4 Conclusions

The resistive transition of nearly single phase $Bi_{1.65}Pb_{0.35}Sr_2Ca_2Cu_3O_{10+\delta}$ samples subjected to different uniaxial compacting pressure, have been investigated under low applied magnetic fields ($B_a < 20$ mT). We have found that the dissipation region between the offset temperature, T_{off}, and the onset temperature, T_{on}, are very sensitive to the applied magnetic field and the uniaxial compacting pressure. The obtained results assure that increasing the uniaxial compacting pressure improves both the grain connectivity and the texture degree of samples. Values of Lotgering factor along the $(00l)$ direction were estimated from X-ray diffraction patterns and indicate that the texture degree increases ∼30% between samples **BP2** ($P = 99$ MPa) and **BP5** ($P = 247$ MPa). We have also found that the above changes in the texture degree of samples are reflected in the intergranular pinning energy of the samples. An estimate of the effective intergranular pinning energy, by using the the thermally activated flux-creep model, reveals that at $B_a = 1$ mT, U_0 increases ∼75% between **BP2** and **BP5** samples. However, at $B_a = 8$ mT the relative value is around ∼14%. The above results in combination with an increase of ∼90% in the $J_c(0)$, assure that increasing uniaxial compacting pressure improves the intergranular properties of Bi-2223 ceramic samples. In addition, we have observed a different behavior of the $U_0(H)$ dependence, in all samples, for applied magnetic fields lower than 8 mT. We have suggested that such differences can be related to the existence of different superconducting levels within the samples at the intergranular region: the superconducting grains, the weak-links and the superconducting clusters.

This work was supported by the Brazilian agency Fundação de Amparo à Pesquisa do Estado de São Paulo (FAPESP) under Grant No. 05/53241-9. One of us E.G-A. is FAPESP fellow under Grant No. 06/50192-0. R.F.J. is a Conselho Nacional de Desenvolvimento Científico e Tecnológico (CNPq) fellow under Grant No. 303272/2004-0.

References

1. M. Tinkham, Phys. Rev. Lett. **61**, 1658 (1988)
2. T.T. Palstra, B. Batlogg, R.B. van Dover, L.F. Scheemeyer, J.V. Waszczak, Appl. Phys. Lett. **54**, 763 (1989)
3. D.H. Kim, K.F. Gray, R.T. Kampwirth, D.M. Mckay, Phys. Rev. B **42**, 6249 (1990)
4. G.L. Bhalla, Pratima, Amita Malik, K.K. Singh, Physica C **391**, 17 (2003)
5. G.L. Bhalla, Pratima, Physica C **406**, 154 (2004)
6. M. Charalambous, J. Chaussy, P. Lejay, Phys. Rev. B **45**, 5091 (1992)
7. X.J. Xu, L. Fu, L.B. Wang, Y.H. Zhang, J. Fang, X.W. Cao XW, K.B. Li, S. Hisashi, Phys. Rev. B **59**, 608 (1999)
8. A. Salem, G. Jakob, H. Adrian, Physica C **402**, 354 (2004)
9. K.A. Müller, M. Takashige, J.G. Bednorz, Phys. Rev. Lett. **58**, 1143 (1987)
10. V. Ambegaokar, B.I. Halperin, Phys. Rev. Lett. **22**, 1364 (1969)
11. J.M. Kosterlitz, D.J. Thouless, J. Phys. C **6**, 1181 (1973)
12. P.W. Anderson, Y.B. Kim, Rev. Mod. Phys. **36**, 39 (1964)
13. H. Hilgenkamp, J. Mannhart, Rev. Mod. Phys. **74**, 485 (2002)
14. T.T. Tan, S. Li, H. Cooper, W. Gao, H.K. Liu, S.X. Dou, Supercond. Sci. Technol. **14**, 471 (2001)
15. P. Muné, E. Govea-Alcaide, R.F. Jardim, Physica C **384**, 491 (2003)
16. J. Albrecht, Ch. Jooss, R. Warthmann, A. Forkl, H. Kronmüller, Phys. Rev. B **57**, 10332 (1998)
17. A. Gurevich, M.S. Rzchowski1, G. Daniels, S. Patnaik, B.M. Hinaus, F. Carillo, F. Tafuri, D.C. Larbalestier, Phys. Rev. Lett. **88**, 097001 (2002)
18. V.N. Viera, J.P. da Silva, J. Schaf, Phys. Rev. B **64**, 094516 (2001)
19. Y. Yeshurun, A.P. Malozemoff, Phys. Rev. Lett. **60**, 2220 (1988)
20. D. Pandey, R. Mahesh, A.K. Singh, V.S. Tiwari, Physica C **184**, 135 (1991)
21. E. Govea-Alcaide, R.F. Jardim, P. Muné, Physica C **423**, 152 (2005)
22. E. Govea-Alcaide, P. Muné, R.F. Jardim, Brazilian J. Phys. **35**, 680 (2005)
23. E. Govea-Alcaide, R.F. Jardim, P. Muné, Phys. Stat. Sol. a **202**, 2484 (2005)
24. T. Kobayashi, R. Ogawa, K. Miyazawa, M. Kuwabara, J. Mater. Res. **17**, 79 (2000)
25. S.A. Salem, Physica C **444**, 40 (2006)
26. H.S. Gamchi, G.J. Russell, K.N.R. Taylor, Phys. Rev. B **50**, 12950 (1994)